Hello Edge: Keyword Spotting on Microcontrollers

Yundong Zhang[1,2], Naveen Suda[1], Liangzhen Lai[1] and Vikas Chandra[1]

[1]Arm, San Jose, CA
[2]Stanford University, Stanford, CA

Abstract

Keyword spotting (KWS) is a critical component for enabling speech based user interactions on smart devices. It requires real-time response and high accuracy for good user experience. Recently, neural networks have become an attractive choice for KWS architecture because of their superior accuracy compared to traditional speech processing algorithms. Due to its always-on nature, KWS application has highly constrained power budget and typically runs on tiny microcontrollers with limited memory and compute capability. The design of neural network architecture for KWS must consider these constraints. In this work, we perform neural network architecture evaluation and exploration for running KWS on resource-constrained microcontrollers. We train various neural network architectures for keyword spotting published in literature to compare their accuracy and memory/compute requirements. We show that it is possible to optimize these neural network architectures to fit within the memory and compute constraints of microcontrollers without sacrificing accuracy. We further explore the depthwise separable convolutional neural network (DS-CNN) and compare it against other neural network architectures. DS-CNN achieves an accuracy of 95.4%, which is ~10% higher than the DNN model with similar number of parameters.

1 Introduction

Deep learning algorithms have evolved to a stage where they have surpassed human accuracies in a variety of cognitive tasks including image classification [1] and conversational speech recognition [2]. Motivated by the recent breakthroughs in deep learning based speech recognition technologies, speech is increasingly becoming a more natural way to interact with consumer electronic devices, for example, Amazon Echo, Google Home and smart phones. However, always-on speech recognition is not energy-efficient and may also cause network congestion to transmit continuous audio stream from billions of these devices to the cloud. Furthermore, such a cloud based solution adds latency to the application, which hurts user experience. There are also privacy concerns when audio is continuously transmitted to the cloud. To mitigate these concerns, the devices first detect predefined keyword(s) such as "Alexa", "Ok Google", "Hey Siri", etc., which is commonly known as keyword spotting (KWS). Detection of keyword wakes up the device and then activates the full scale speech recognition either on device [3] or in the cloud. In some applications, the sequence of keywords can be used as voice commands to a smart device such as a voice-enabled light bulb. Since KWS system is always-on, it should have very low power consumption to maximize battery life. On the other hand, the KWS system should detect the keywords with high accuracy and low latency, for best user experience. These conflicting system requirements make KWS an active area of research ever since its inception over 50 years ago [4]. Recently, with the renaissance of artificial neural networks in the form of deep learning algorithms, neural network (NN) based KWS has become very popular [5, 6, 7, 8].

[2]Work was done while the author was an intern at Arm.

Low power consumption requirement for keyword spotting systems make microcontrollers an obvious choice for deploying KWS in an always-on system. Microcontrollers are low-cost energy-efficient processors that are ubiquitous in our everyday life with their presence in a variety of devices ranging from home appliances, automobiles and consumer electronics to wearables. However, deployment of neural network based KWS on microcontrollers comes with following challenges:

Limited memory footprint: Typical microcontroller systems have only tens to few hundred KB of memory available. The entire neural network model, including input/output, weights and activations, has to fit within this small memory budget.

Limited compute resources: Since KWS is always-on, the real-time requirement limits the total number of operations per neural network inference.

These microcontroller resource constraints in conjunction with the high accuracy and low latency requirements of KWS call for a resource-constrained neural network architecture exploration to find *lean* neural network structures suitable for KWS, which is the primary focus of our work. The main contributions of this work are as follows:

- We first train the popular KWS neural net models from the literature [5, 6, 7, 8] on Google speech commands dataset [9] and compare them in terms of accuracy, memory footprint and number of operations per inference.
- In addition, we implement a new KWS model using depth-wise separable convolutions and point-wise convolutions, inspired by the success of resource-efficient MobileNet [10] in computer vision. This model outperforms the other prior models in all aspects of accuracy, model size and number of operations.
- Finally, we perform resource-constrained neural network architecture exploration and present comprehensive comparison of different network architectures within a set of compute and memory constraints of typical microcontrollers. The code, model definitions and pretrained models are available at https://github.com/ARM-software/ML-KWS-for-MCU.

2 Background

2.1 Keyword Spotting (KWS) System

A typical KWS system consists of a feature extractor and a neural network based classifier as shown in Fig. 1. First, the input speech signal of length L is framed into overlapping frames of length l with a stride s, giving a total of $T = \frac{L-l}{s} + 1$ frames. From each frame, F speech features are extracted, generating a total of $T \times F$ features for the entire input speech signal of length L. Log-mel filter bank energies (LFBE) and Mel-frequency cepstral coefficients (MFCC) are the commonly used human-engineered speech features in deep learning based speech-recognition, that are adapted from traditional speech processing techniques. Feature extraction using LFBE or MFCC involves translating the time-domain speech signal into a set of frequency-domain spectral coefficients, which enables dimensionality compression of the input signal. The extracted speech feature matrix is fed into a classifier module, which generates the probabilities for the output classes. In a real-world scenario where keywords need to be identified from a continuous audio stream, a posterior handling module averages the output probabilities of each output class over a period of time, improving the overall confidence of the prediction.

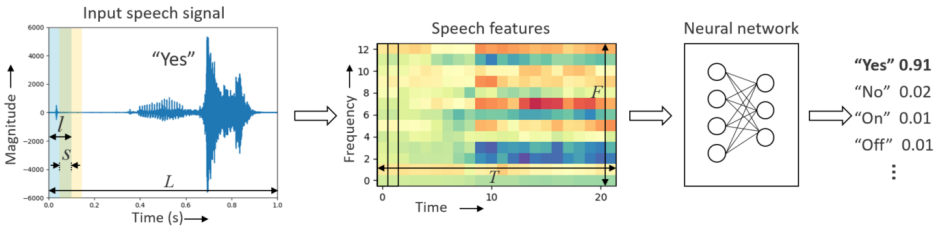

Figure 1: Keyword spotting pipeline.

Traditional speech recognition technologies for KWS use Hidden Markov Models (HMMs) and Viterbi decoding [11, 12]. While these approaches achieve reasonable accuracies, they are hard to train and are computationally expensive during inference. Other techniques explored for KWS include discriminative models adopting a large-margin problem formulation [13] or recurrent neural networks (RNN) [14]. Although these methods significantly outperform HMM based KWS in terms of accuracy, they suffer from large detection latency. KWS models using deep neural networks (DNN) based on fully-connected layers with rectified linear unit (ReLU) activation functions are introduced in [5], which outperforms the HMM models with a very small detection latency. Furthermore, low-rank approximation techniques are used to compress the DNN model weights achieving similar accuracy with less hardware resources [15, 16]. The main drawback of DNNs is that they ignore the local temporal and spectral correlation in the input speech features. In order to exploit these correlations, different variants of convolutional neural network (CNN) based KWS are explored in [6], which demonstrate higher accuracy than DNNs. The drawback of CNNs in modeling time varying signals (e.g. speech) is that they ignore long term temporal dependencies. Combining the strengths of CNNs and RNNs, convolutional recurrent neural network based KWS is investigated in [7] and demonstrate the robustness of the model to noise. While all the prior KWS neural networks are trained with cross entropy loss function, a max-pooling based loss function for training KWS model with long short-term memory (LSTM) is proposed in [8], which achieves better accuracy than the DNNs and LSTMs trained with cross entropy loss.

Although many neural network models for KWS are presented in literature, it is difficult to make a fair comparison between them as they are all trained and evaluated on different proprietary datasets (e.g. "TalkType" dataset in [7], "Alexa" dataset in [8], etc.) with different input speech features and audio duration. Also, the primary focus of prior research has been to maximize the accuracy with a small memory footprint model, without explicit constraints of underlying hardware, such as limits on number of operations per inference. In contrast, this work is more hardware-centric and targeted towards neural network architectures that maximize accuracy on microcontroller devices. The constraints on memory and compute significantly limit the neural network parameters and the number of operations.

2.2 Microcontroller Systems

A typical microcontroller system consists of a processor core, an on-chip SRAM block and an on-chip embedded flash. Table 1 shows some commercially available microcontroller development boards with Arm Cortex-M processor cores with different compute capabilities running at different frequencies (16 MHz to 216 MHz), consisting of a wide range of on-chip memory (SRAM: 8 KB to 320 KB; Flash: 128 KB to 1 MB). The program binary, usually preloaded into the non-volatile flash, is loaded into the SRAM at startup and the processor runs the program with the SRAM as the main data memory. Therefore, the size of the SRAM limits the size of memory that the software can use.

Other than the memory footprint, performance (i.e., operations per second) is also a constraining factor for running neural networks on microcontrollers. Most microcontrollers are designed for embedded applications with low cost and high energy-efficiency as the primary targets, and do not have high throughput for compute-intensive workloads such as neural networks. Some microcontrollers have integrated DSP instructions that can be useful for running neural network workloads. For example, Cortex-M4 and Cortex-M7 have integrated SIMD and MAC instructions that can be used to accelerate low-precision computation in neural networks.

Arm Mbed™ platform	Processor	Frequency	SRAM	Flash
Mbed LPC11U24	Cortex-M0	48 MHz	8 KB	32 KB
Nordic nRF51-DK	Cortex-M0	16 MHz	32 KB	256 KB
Mbed LPC1768	Cortex-M3	96 MHz	32 KB	512 KB
Nucleo F103RB	Cortex-M3	72 MHz	20 KB	128 KB
Nucleo L476RG	Cortex-M4	80 MHz	128 KB	1 MB
Nucleo F411RE	Cortex-M4	100 MHz	128 KB	512 KB
FRDM-K64F	Cortex-M4	120 MHz	256 KB	1 MB
Nucleo F746ZG	Cortex M7	216 MHz	320 KB	1 MB

Table 1: Typical off the shelf Arm Cortex-M based microcontroller development platforms.

3 Neural Network Architectures for KWS

This section gives an overview of all the different neural network architectures explored in this work including the deep neural network (DNN), convolutional neural network (CNN), recurrent neural network (RNN), convolutional recurrent neural network (CRNN) and depthwise separable convolutional neural network (DS-CNN).

3.1 Deep Neural Network (DNN)

The DNN is a standard feed-forward neural network made of a stack of fully-connected layers and non-linear activation layers. The input to the DNN is the flattened feature matrix, which feeds into a stack of d hidden fully-connected layers each with n neurons. Typically, each fully-connected layer is followed by a rectified linear unit (ReLU) based activation function. At the output is a linear layer followed by a softmax layer generating the output probabilities of the k keywords, which are used for further posterior handling.

3.2 Convolutional Neural Network (CNN)

One main drawback of DNN based KWS is that they fail to efficiently model the local temporal and spectral correlation in the speech features. CNNs exploit this correlation by treating the input time-domain and spectral-domain features as an image and performing 2-D convolution operations over it. The convolution layers are typically followed by batch normalization [17], ReLU based activation functions and optional max/average pooling layers, which reduce the dimensionality of the features. During inference, the parameters of batch normalization can be folded into the weights of the convolution layers. In some cases, a linear low-rank layer, which is simply a fully-connected layer without non-linear activation, is added in between the convolution layers and dense layers for the purpose of reducing parameters and accelerating training [18, 19].

3.3 Recurrent Neural Network (RNN)

RNNs have shown superior performance in many sequence modeling tasks, especially speech recognition [20], language modeling [21], translation [22], etc. RNNs not only exploit the temporal relation between the input signal, but also capture the long-term dependencies using "gating" mechanism. Unlike CNNs where input features are treated as 2-D image, RNNs operate for T time steps, where at each time step t the corresponding spectral feature vector $f_t \in R^F$ concatenated with the previous time step output h_{t-1} is used as input to the RNN. Figure 2 shows the model architecture of a typical RNN model, where the RNN cell could be an LSTM cell [23, 24] or a gated recurrent unit (GRU) cell [25, 26]. Since the weights are reused across all the T time steps, the RNN models tend to have less number of parameters compared to the CNNs. Similar to batch normalization in CNNs, research show that applying layer normalization can be beneficial for training RNNs [27], in which the hidden states are normalized during each time step.

3.4 Convolutional Recurrent Neural Network (CRNN)

Convolution recurrent neural network [7] is a hybrid of CNN and RNN, which takes advantages of both. It exploits the local temporal/spatial correlation using convolution layers and global temporal dependencies in the speech features using recurrent layers. As shown in Fig. 3, a CRNN model

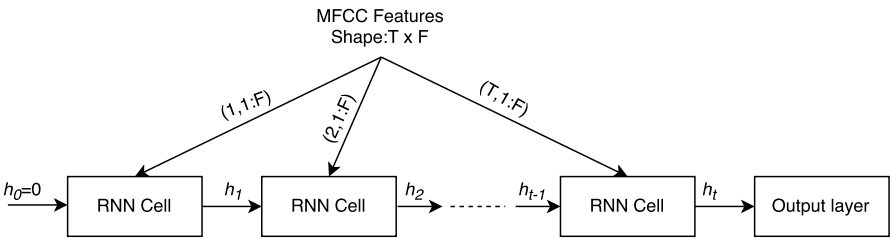

Figure 2: Model architecture of RNN.

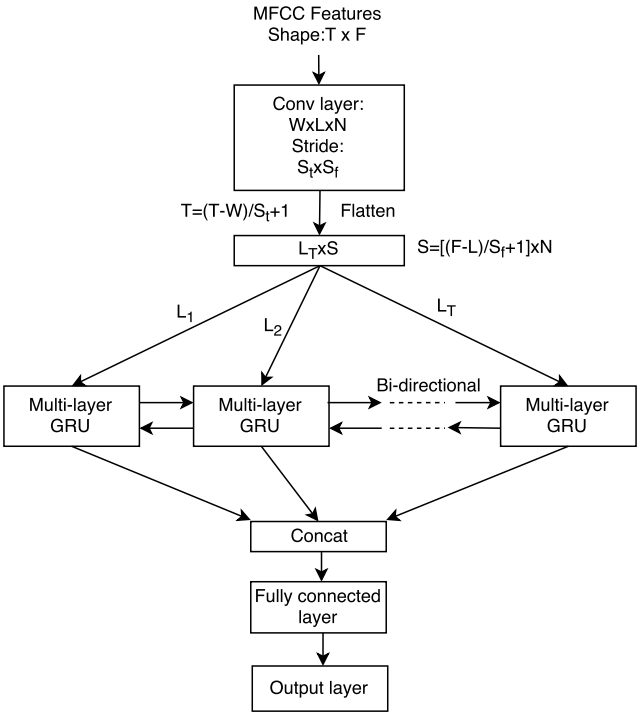

Figure 3: Model Architecture of CRNN.

starts with a convolution layer, followed by an RNN to encode the signal and a dense fully-connected layer to map the information. Here, the recurrent layer is bi-directional [28] and has multiple stages, increasing the network learning capability. Gated recurrent units (GRU) [25] is used as the base cell for recurrent layers, as it uses fewer parameters than LSTMs and gave better convergence in our experiments.

3.5 Depthwise Separable Convolutional Neural Network (DS-CNN)

Recently, depthwise separable convolution has been proposed as an efficient alternative to the standard 3-D convolution operation [29] and has been used to achieve compact network architectures in the area of computer vision [10, 30]. DS-CNN first convolves each channel in the input feature map with a separate 2-D filter and then uses pointwise convolutions (i.e. $1x1$) to combine the outputs in the depth dimension. By decomposing the standard 3-D convolutions into 2-D convolutions followed by 1-D convolutions, depthwise separable convolutions are more efficient both in number of parameters and operations, which makes deeper and wider architecture possible even in the resource-constrained microcontroller devices. In this work, we adopt a depthwise separable CNN based on the implementation of MobileNet [10] as shown in Fig. 4. An average pooling followed by a fully-connected layer is used at the end to provide global interaction and reduce the total number of parameters in the final layer.

4 Experiments and Results

We use the Google speech commands dataset [9] for the neural network architecture exploration experiments. The dataset consists of 65K 1-second long audio clips of 30 keywords, by thousands of different people, with each clip consisting of only one keyword. The neural network models are trained to classify the incoming audio into one of the 10 keywords - "Yes", "No", "Up", "Down", "Left", "Right", "On", "Off", "Stop", "Go", along with "silence" (i.e. no word spoken) and "unknown" word, which is the remaining 20 keywords from the dataset. The dataset is split into training, validation and test set in the ratio of 80:10:10 while making sure that the audio clips from the same person stays in the same set. All models are trained in Google Tensorflow framework [31] using

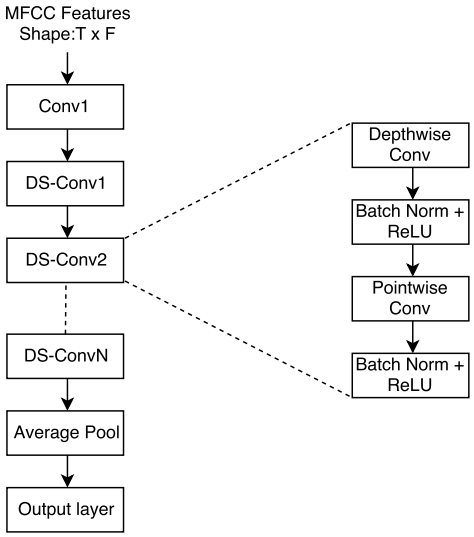

Figure 4: Depthwise separable CNN architecture.

the standard cross-entropy loss and Adam optimizer [32]. With a batch size of 100, the models are trained for 20K iterations with initial learning rate of 5×10^{-4}, and reduced to 10^{-4} after first 10K iterations. The training data is augmented with background noise and random time shift of up to 100ms. The trained models are evaluated based on the classification accuracy on the test set.

4.1 Training Results

Table 2 summarizes the accuracy, memory requirement and operations per inference for the network architectures for KWS from literature [5, 6, 7, 8] trained on Google speech commands dataset [9]. For all the models, we use 40 MFCC features extracted from a speech frame of length 40ms with a stride of 20ms, which gives 1960 (49×40) features for 1 second of audio. The accuracy shown in the table is the accuracy on test set. The memory shown in the table assumes 8-bit weights and activations, which is sufficient to achieve same accuracy as that from a full-precision network.

NN Architecture	Accuracy	Memory	Operations
DNN [5]	84.3%	288 KB	0.57 MOps
CNN-1 [6]	90.7%	556 KB	76.02 MOps
CNN-2 [6]	84.6%	149 KB	1.46 MOps
LSTM [8]	88.8%	26 KB	2.06 MOps
CRNN [7]	87.8%	298 KB	5.85 MOps

Table 2: Neural network model accuracy. CNN-1, CNN-2 are (*cnn-trad-fpool3, cnn-one-fstride4*) architectures from [6].

Also, we assume that the memory for activations is reused across different layers and hence memory requirement for the activations uses the maximum of two consecutive layers. The operations in the table counts the total number of multiplications and additions in the matrix-multiplication operations in each layer in the network, which is representative of the execution time of the entire network. The models from the existing literature are optimized for different datasets and use different memory/compute resources, hence a direct comparison of accuracy is unfair. That said, these results still provide useful insights on the different neural network architectures for KWS:

- Although DNNs do not achieve the best accuracy and tend to be memory intensive, they have less number of operations/inference and hence suit well to systems that have limited compute capability (e.g. systems running at low operating frequencies for energy-efficiency).
- CNNs, on the other hand, achieve higher accuracy than DNNs but at the cost of large number of operations and/or memory requirement.

- LSTMs and CRNNs achieve a balance between memory and operations while still achieving good accuracy.

4.2 Classifying Neural Networks for KWS based on Resource Requirements

As discussed in section 2.2, memory footprint and execution time are the two important considerations in being able to run keyword spotting on microcontrollers. These should be considered when designing and optimizing neural networks for running keyword spotting. Based on typical microcontroller system configurations (as described in Table 1), we derive three sets of constraints for the neural networks in Table 3, targeting small, medium and large microcontroller systems. Both memory and compute limit are derived with assumptions that some amount of resources will be allocated for running other tasks such as OS, I/O, network communication, etc. The operations per inference limit assumes that the system is running 10 inferences per second.

NN size	NN memory limit	Ops/inference limit
Small (S)	80 KB	6 MOps
Medium (M)	200 KB	20 MOps
Large (L)	500 KB	80 MOps

Table 3: Neural network (NN) classes for KWS models considered in this work, assuming 10 inferences per second and 8-bit weights/activations.

4.3 Resource Constrained Neural Network Architecture Exploration

Figure 5 shows the number of operations per inference, memory requirement and test accuracy of neural network models from prior work [5, 6, 7, 8] trained on Google speech commands dataset overlayed with the memory and compute bounding boxes for the neural network classes from section 4.2. An ideal model would have high accuracy, small memory footprint and lower number of computations, i.e., close to the origin in Fig. 5. Apart from the LSTM model, the other models are too memory/compute resource heavy and do not fit into the bounding box *S* with 80KB/6MOps memory/compute limits. CNN-2, CRNN and DNN models fit in the *M* and *L* bounding boxes, but have lower accuracies as compared to the CNN-1 model, which does not fit in any of the boxes at all. The rest of this section discusses different hyperparameters of the feature extraction and neural network architectures that can be tuned in order to bring the models close to the origin and still achieve high accuracy.

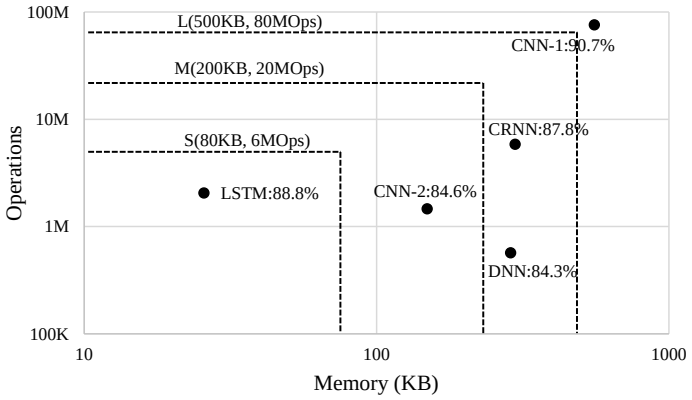

Figure 5: Number of operations vs. memory vs. test accuracy of NN models from prior work [5, 6, 7, 8] trained on the speech commands dataset [9].

As shown in Fig. 1, from each input speech signal, $T \times F$ features are extracted and the number of these features impact the model size, number of operations and accuracy. The key parameters in the feature extraction step that impact the model size, number of operations and accuracy are (1) number of MFCC features per frame (F) and (2) the frame stride (S). The number of MFCC features per audio frame (F) impacts the number of weights in fully-connected and recurrent layers,

but not in convolution layers as weights are reused in convolution layers. The frame stride (S), which determines the number of frames to be processed per inference (i.e. T), impacts the number of weights in fully-connected layers but not in recurrent and convolution layers because of the weight reuse. Both F and S impact the number of operations per inference. An efficient model would maximize accuracy using small $T \times F$, i.e., small F and/or large S.

The neural network architectures and the corresponding hyperparameters explored in this work are summarized in Table 4. The LSTM model mentioned in the table includes peephole connections and output projection layer similar to that in [8], whereas basic LSTM model does not include those. CRNN uses one convolution layer followed by multi-layer GRU for the recurrent layers. We also use batch normalization for convolutional/fully-connected layers and layer normalization for recurrent layers. During inference, the parameters of batch normalization and layer normalization can be folded into the weights of the convolution or recurrent layers and hence these layers are ignored in memory/Ops computation.

NN model	Model hyperparameters
DNN	Number of fully-connected (FC) layers and size of each FC layer
CNN	Number of Conv layers: features/kernel size/stride, linear layer dim., FC layer size
Basic LSTM	Number of memory cells
LSTM	Number of memory cells, projection layer size
GRU	Number of memory cells
CRNN	Conv features/kernel size/stride, Number of GRU and memory cells, FC layer size
DS-CNN	Number of DS-Conv layers, DS-Conv features/kernel size/stride

Table 4: Neural network hyperparameters used in this study.

We iteratively perform exhaustive search of feature extraction hyperparameters and NN model hyperparameters followed by manual selection to narrow down the search space. The final best performing models for each neural network architecture along with their memory requirements and operations are summarized in Table 5 and Fig. 6. The hyperparameters of these networks are summarized in Appendix A. From the results we can see that DNNs are memory-bound and achieve less accuracies and saturate at ~87% even when the model is scaled up. CNNs achieve better accuracies than DNN, but are limited by the weights in the final fully-connected layers. RNN models (i.e. Basic LSTM, LSTM and GRU) achieve better accuracies than CNNs and yield even smaller models with less Ops in some cases, demonstrating that exploiting temporal dependencies maximizes accuracy within the same resource budget. CRNN models, which combine the best properties of CNNs and RNNs, achieve better accuracies than both CNNs and RNNs, even with less Ops. CRNN architecture also scales up well when more memory/compute resources are available. DS-CNN achieves the best accuracies and demonstrate good scalability owing to their deeper architecture enabled by depthwise separable convolution layers, which are less compute/memory intensive.

NN model	S(80KB, 6MOps)			M(200KB, 20MOps)			L(500KB, 80MOps)		
	Acc.	Mem.	Ops	Acc.	Mem.	Ops	Acc.	Mem.	Ops
DNN	84.6%	80.0KB	158.8K	86.4%	199.4KB	397.0K	86.7%	496.6KB	990.2K
CNN	91.6%	79.0KB	5.0M	92.2%	199.4KB	17.3M	92.7%	497.8KB	25.3M
Basic LSTM	92.0%	63.3KB	5.9M	93.0%	196.5KB	18.9M	93.4%	494.5KB	47.9M
LSTM	92.9%	79.5KB	3.9M	93.9%	198.6KB	19.2M	94.8%	498.8KB	48.4M
GRU	93.5%	78.8KB	3.8M	94.2%	200.0KB	19.2M	94.7%	499.7KB	48.4M
CRNN	94.0%	79.7KB	3.0M	94.4%	199.8KB	7.6M	95.0%	499.5KB	19.3M
DS-CNN	94.4%	38.6KB	5.4M	94.9%	189.2KB	19.8M	95.4%	497.6KB	56.9M

Table 5: Summary of best neural networks from the hyperparameter search. The memory required for storing the 8-bit weights and activations is shown in the table.

To study the scalability of the models for smaller microcontroller systems with memory as low as 8KB, we expand the search space for DS-CNN models. Figure 7 shows the accuracy, memory/Ops requirements of the DS-CNN models targeted for such constrained devices. It shows that scaled-down DS-CNN models achieve better accuracies than DNN models with similar number of Ops, but with >10x reduction in memory requirement.

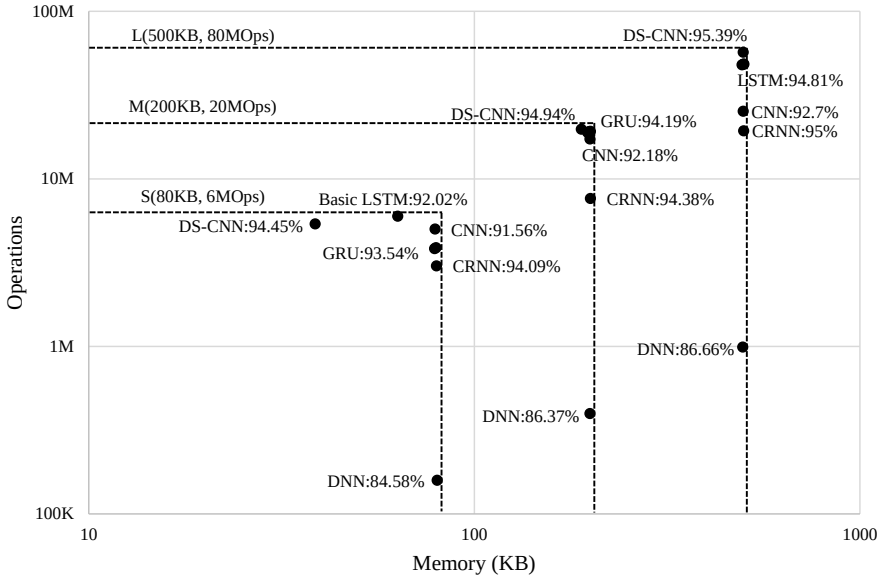

Figure 6: Memory vs. Ops/inference of the best models described in Table 5.

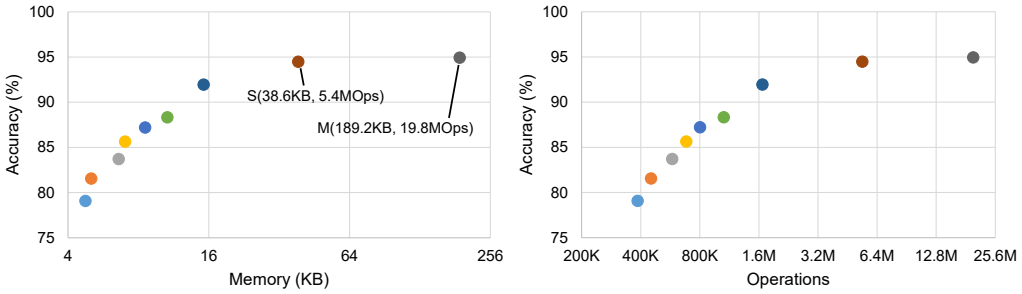

Figure 7: Accuracy vs. memory and Ops of different DS-CNN models demonstrating the scalability of DS-CNN models down to <8KB memory footprint and <500K operations.

4.4 Neural Network Quantization

Neural networks are typically trained with floating point weights and activations. Previous research [33, 34, 35] have shown that fixed-point weights is sufficient to run neural networks with minimal loss in accuracy. Microcontroller systems have limited memory, which motivates the quantization of 32-bit floating point weights to 8-bit fixed point weights for deployment, thus reducing the model size by 4×. Moreover, fixed-point integer operations run much faster than floating point operations in typical microcontrollers, which is another reason for executing quantized model during deployment.

In this work, we use the quantization flow described in [34] using 8-bits to represent all the weights and activations. For a given signed 2's complement 8-bit fixed-point number, its value (v) can be expressed as $v = -B_7.2^{7-N} + \sum_{i=0}^{6} B_i.2^{i-N}$, where N is the fractional length, which can also be negative. N is fixed for a given layer, but can be different in other layers. For example, $N = 0$ can represent the range $[-128, 127]$ with a step of 1, $N = 7$ can represent the range $[-1, 1 - (1/2^7)]$ with a step of $1/2^7$ and $N = -2$ can represent the range $[-512, 508]$ with a step of 2^2.

The weights are quantized to 8-bits progressively one layer at a time by finding the optimal N for each layer that minimizes the loss in accuracy because of quantization. After all the weights are quantized, the activations are also quantized in a similar way to find the appropriate fractional length N for each layer. Table 6 shows the accuracies of representative 8-bit networks quantized using this method and compared with those of the original full-precision networks. The table shows that the

accuracy of the quantized network is either same or marginally better than the full-precision network, possibly due to better regularization because of quantization. We believe that the same conclusion will hold for the other neural network models explored in this work.

NN model	32-bit floating point model accuracy			8-bit quantized model accuracy		
	Train	Val.	Test	Train	Val.	Test
DNN	97.77%	88.04%	86.66%	97.99%	88.91%	87.60%
Basic LSTM	98.38%	92.69%	93.41%	98.21%	92.53%	93.51%
GRU	99.23%	93.92%	94.68%	99.21%	93.66%	94.68%
CRNN	98.34%	93.99%	95.00%	98.43%	94.08%	95.03%

Table 6: Accuracy comparison of representative 8-bit quantized networks with full-precision networks.

4.5 KWS Deployment on Microcontroller

We deployed the KWS application on Cortex-M7 based STM32F746G-DISCO development board using CMSIS-NN kernels [36]. A picture of the board performing KWS is shown in Fig. 8. The deployed model is a DNN model with 8-bit weights and 8-bit activations and KWS is running at 10 inferences per second. Each inference, including memory copying, MFCC feature extraction and DNN execution, takes about 12 ms. The microcontroller can be put into Wait-for-Interrupt (WFI) mode for the remaining time for power saving. The entire KWS application occupies ~70 KB memory, including ~66 KB for weights, ~1 KB for activations and ~ 2 KB for audio I/O and MFCC features.

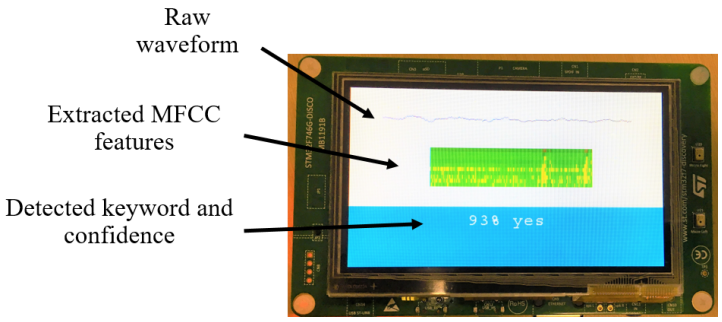

Figure 8: Deployment of KWS on Cortex-M7 development board.

5 Conclusions

Hardware optimized neural network architecture is key to get efficient results on memory and compute constrained microcontrollers. We trained various neural network architectures for keyword spotting published in literature on Google speech commands dataset to compare their accuracy and memory requirements vs. operations per inference, from the perspective of deployment on microcontroller systems. We quantized representative trained 32-bit floating-point KWS models into 8-bit fixed-point versions demonstrating that these models can easily be quantized for deployment without any loss in accuracy, even without retraining. Furthermore, we trained a new KWS model using depthwise separable convolution layers, inspired from MobileNet. Based on typical microcontroller systems, we derived three sets of memory/compute constraints for the neural networks and performed resource constrained neural network architecture exploration to find the best networks achieving maximum accuracy within these constraints. In all three sets of memory/compute constraints, depthwise separable CNN model (DS-CNN) achieves the best accuracies of 94.4%, 94.9% and 95.4% compared to the other model architectures within those constraints, which shows good scalability of the DS-CNN model. The code, model definitions and pretrained models are available at https://github.com/ARM-software/ML-KWS-for-MCU.

Acknowledgements

We would like to thank Matt Mattina from Arm Research and Ian Bratt from Arm ML technology group for their help and support. We would also like to thank Pete Warden from Google's TensorFlow team for his valuable inputs and feedback on this project.

References

[1] Yunpeng Chen, Jianan Li, Huaxin Xiao, Xiaojie Jin, Shuicheng Yan, and Jiashi Feng. Dual path networks. *arXiv preprint arXiv:1707.01629*, 2017.

[2] W. Xiong, L. Wu, F. Alleva, Jasha Droppo, X. Huang, and Andreas Stolcke. The microsoft 2017 conversational speech recognition system. *CoRR*, abs/1708.06073, 2017.

[3] Ian McGraw, Rohit Prabhavalkar, Raziel Alvarez, Montse Gonzalez Arenas, Kanishka Rao, David Rybach, Ouais Alsharif, Haşim Sak, Alexander Gruenstein, Françoise Beaufays, et al. Personalized speech recognition on mobile devices. In *Acoustics, Speech and Signal Processing (ICASSP), 2016 IEEE International Conference on*, pages 5955–5959. IEEE, 2016.

[4] C Teacher, H Kellett, and L Focht. Experimental, limited vocabulary, speech recognizer. *IEEE Transactions on Audio and Electroacoustics*, 15(3):127–130, 1967.

[5] Guoguo Chen, Carolina Parada, and Georg Heigold. Small-footprint keyword spotting using deep neural networks. In *Acoustics, Speech and Signal Processing (ICASSP), 2014 IEEE International Conference on*, pages 4087–4091. IEEE, 2014.

[6] Tara N Sainath and Carolina Parada. Convolutional neural networks for small-footprint keyword spotting. In *Sixteenth Annual Conference of the International Speech Communication Association*, 2015.

[7] Sercan O Arik, Markus Kliegl, Rewon Child, Joel Hestness, Andrew Gibiansky, Chris Fougner, Ryan Prenger, and Adam Coates. Convolutional recurrent neural networks for small-footprint keyword spotting. *arXiv preprint arXiv:1703.05390*, 2017.

[8] Ming Sun, Anirudh Raju, George Tucker, Sankaran Panchapagesan, Gengshen Fu, Arindam Mandal, Spyros Matsoukas, Nikko Strom, and Shiv Vitaladevuni. Max-pooling loss training of long short-term memory networks for small-footprint keyword spotting. In *Spoken Language Technology Workshop (SLT), 2016 IEEE*, pages 474–480. IEEE, 2016.

[9] Pete Warden. Speech commands: A public dataset for single-word speech recognition. *Dataset available from http://download.tensorflow.org/data/speech_commands_v0.01.tar.gz*, 2017.

[10] Andrew G Howard, Menglong Zhu, Bo Chen, Dmitry Kalenichenko, Weijun Wang, Tobias Weyand, Marco Andreetto, and Hartwig Adam. Mobilenets: Efficient convolutional neural networks for mobile vision applications. *arXiv preprint arXiv:1704.04861*, 2017.

[11] Jay G Wilpon, Lawrence R Rabiner, C-H Lee, and ER Goldman. Automatic recognition of keywords in unconstrained speech using hidden markov models. *IEEE Transactions on Acoustics, Speech, and Signal Processing*, 38(11):1870–1878, 1990.

[12] Richard C Rose and Douglas B Paul. A hidden markov model based keyword recognition system. In *Acoustics, Speech, and Signal Processing, 1990. ICASSP-90., 1990 International Conference on*, pages 129–132. IEEE, 1990.

[13] Joseph Keshet, David Grangier, and Samy Bengio. Discriminative keyword spotting. *Speech Communication*, 51(4):317–329, 2009.

[14] Santiago Fernández, Alex Graves, and Jürgen Schmidhuber. An application of recurrent neural networks to discriminative keyword spotting. *Artificial Neural Networks–ICANN 2007*, pages 220–229, 2007.

[15] George Tucker, Minhua Wu, Ming Sun, Sankaran Panchapagesan, Gengshen Fu, and Shiv Vitaladevuni. Model compression applied to small-footprint keyword spotting. In *INTERSPEECH*, pages 1878–1882, 2016.

[16] Preetum Nakkiran, Raziel Alvarez, Rohit Prabhavalkar, and Carolina Parada. Compressing deep neural networks using a rank-constrained topology. In *INTERSPEECH*, pages 1473–1477, 2015.

[17] Sergey Ioffe and Christian Szegedy. Batch normalization: Accelerating deep network training by reducing internal covariate shift. In *International Conference on Machine Learning*, pages 448–456, 2015.

[18] Jimmy Ba and Rich Caruana. Do deep nets really need to be deep? In *Advances in neural information processing systems*, pages 2654–2662, 2014.

[19] Tara N Sainath, Brian Kingsbury, Vikas Sindhwani, Ebru Arisoy, and Bhuvana Ramabhadran. Low-rank matrix factorization for deep neural network training with high-dimensional output targets. In *Acoustics, Speech and Signal Processing (ICASSP), 2013 IEEE International Conference on*, pages 6655–6659. IEEE, 2013.

[20] Haşim Sak, Andrew Senior, and Françoise Beaufays. Long short-term memory recurrent neural network architectures for large scale acoustic modeling. In *Fifteenth Annual Conference of the International Speech Communication Association*, 2014.

[21] Tomas Mikolov, Martin Karafiát, Lukas Burget, Jan Cernockỳ, and Sanjeev Khudanpur. Recurrent neural network based language model. In *Interspeech*, volume 2, page 3, 2010.

[22] Ilya Sutskever, Oriol Vinyals, and Quoc V Le. Sequence to sequence learning with neural networks. In *Advances in neural information processing systems*, pages 3104–3112, 2014.

[23] Sepp Hochreiter and Jürgen Schmidhuber. Long short-term memory. *Neural computation*, 9(8):1735–1780, 1997.

[24] Felix A Gers, Nicol N Schraudolph, and Jürgen Schmidhuber. Learning precise timing with lstm recurrent networks. *Journal of machine learning research*, 3(Aug):115–143, 2002.

[25] Kyunghyun Cho, Bart Van Merriënboer, Caglar Gulcehre, Dzmitry Bahdanau, Fethi Bougares, Holger Schwenk, and Yoshua Bengio. Learning phrase representations using rnn encoder-decoder for statistical machine translation. *arXiv preprint arXiv:1406.1078*, 2014.

[26] Junyoung Chung, Caglar Gulcehre, KyungHyun Cho, and Yoshua Bengio. Empirical evaluation of gated recurrent neural networks on sequence modeling. *arXiv preprint arXiv:1412.3555*, 2014.

[27] Jimmy Lei Ba, Jamie Ryan Kiros, and Geoffrey E Hinton. Layer normalization. *arXiv preprint arXiv:1607.06450*, 2016.

[28] Mike Schuster and Kuldip K Paliwal. Bidirectional recurrent neural networks. *IEEE Transactions on Signal Processing*, 45(11):2673–2681, 1997.

[29] François Chollet. Xception: Deep learning with depthwise separable convolutions. *arXiv preprint arXiv:1610.02357*, 2016.

[30] Xiangyu Zhang, Xinyu Zhou, Mengxiao Lin, and Jian Sun. Shufflenet: An extremely efficient convolutional neural network for mobile devices. *arXiv preprint arXiv:1707.01083*, 2017.

[31] Martín Abadi, Ashish Agarwal, Paul Barham, Eugene Brevdo, Zhifeng Chen, Craig Citro, Greg S Corrado, Andy Davis, Jeffrey Dean, Matthieu Devin, et al. Tensorflow: Large-scale machine learning on heterogeneous distributed systems. *arXiv preprint arXiv:1603.04467*, 2016.

[32] Diederik Kingma and Jimmy Ba. Adam: A method for stochastic optimization. *arXiv preprint arXiv:1412.6980*, 2014.

[33] Naveen Suda, Vikas Chandra, Ganesh Dasika, Abinash Mohanty, Yufei Ma, Sarma Vrudhula, Jae-sun Seo, and Yu Cao. Throughput-optimized opencl-based fpga accelerator for large-scale convolutional neural networks. In *Proceedings of the 2016 ACM/SIGDA International Symposium on Field-Programmable Gate Arrays*, pages 16–25. ACM, 2016.

[34] Jiantao Qiu, Jie Wang, Song Yao, Kaiyuan Guo, Boxun Li, Erjin Zhou, Jincheng Yu, Tianqi Tang, Ningyi Xu, Sen Song, et al. Going deeper with embedded fpga platform for convolutional neural network. In *Proceedings of the 2016 ACM/SIGDA International Symposium on Field-Programmable Gate Arrays*, pages 26–35. ACM, 2016.

[35] Liangzhen Lai, Naveen Suda, and Vikas Chandra. Deep convolutional neural network inference with floating-point weights and fixed-point activations. *arXiv preprint arXiv:1703.03073*, 2017.

[36] Liangzhen Lai, Naveen Suda, and Vikas Chandra. CMSIS-NN: Efficient neural network kernels for Arm Cortex-M CPUs. *arXiv preprint arXiv:1801.06601*, 2018.

A Appendix: Neural Network Hyperparameters

Table 7 shows the summary of the hyperparameters of the best neural networks described in Table 5, along with their memory, number of operations and accuracy on training, validation and test sets. All the models use 10 MFCC features, with a frame length (L) of 40ms, where as the frame stride (S) is shown in the table. FC stands for fully-connected layer and the number in the parentheses shows the number of neurons in the fully-connected layer. C stands for convolution layer and the numbers in parentheses correspond to the number of convolution features, kernel sizes in time and frequency axes, strides in time and frequency axes. Although not shown, all the convolution and fully connected layers have a ReLU as activation function. L stands for low-rank linear layer with the number of elements shown in parentheses. The number in the parentheses for $LSTM$ and GRU models correspond to the number of memory elements in those models. DSC is depthwise separable convolution layer (DSConv in Fig. 4) and the number in the parentheses correspond to the number of features, kernel size and stride in both time and frequency axes.

Model	S	NN model hyperparameters	Memory	Ops	Train	Val.	Test
DNN	40	FC(144)-FC(144)-FC(144)	80.0KB	158.8K	91.5%	85.6%	84.6%
DNN	40	FC(256)-FC(256)-FC(256)	199.4KB	397.1K	95.4%	86.7%	86.4%
DNN	40	FC(436)-FC(436)-FC(436)	496.6KB	990.2K	97.8%	88.0%	86.7%
CNN	20	C(28,10,4,1,1)-C(30,10,4,2,1)-L(16)-FC(128)	79.0KB	5.0M	96.9%	91.1%	91.6%
CNN	20	C(64,10,4,1,1)-C(48,10,4,2,1)-L(16)-FC(128)	199.4KB	17.3M	98.6%	92.2%	92.2%
CNN	20	C(60,10,4,1,1)-C(76,10,4,2,1)-L(58)-FC(128)	497.8KB	25.3M	99.0%	92.4%	92.7%
Basic LSTM	20	LSTM(118)	63.3KB	5.9M	98.2%	91.5%	92.0%
Basic LSTM	20	LSTM(214)	196.5KB	18.9M	98.9%	92.0%	93.0%
Basic LSTM	20	LSTM(344)	494.5KB	47.9M	99.1%	93.0%	93.4%
LSTM	40	LSTM(144), Projection(98)	79.5KB	3.9M	98.5%	92.3%	92.9%
LSTM	20	LSTM(280), Projection(130)	198.6KB	19.2M	98.8%	92.9%	93.9%
LSTM	20	LSTM(500), Projection(188)	498.8KB	4.8M	98.9%	93.5%	94.8%
GRU	40	GRU(154)	78.8KB	3.8M	98.4%	92.7%	93.5%
GRU	20	GRU(250)	200.0KB	19.2M	98.9%	93.6%	94.2%
GRU	20	GRU(400)	499.7KB	48.4M	99.2%	93.9%	93.7%
CRNN	20	C(48,10,4,2,2)-GRU(60)-GRU(60)-FC(84)	79.8KB	3.0M	98.4%	93.6%	94.1%
CRNN	20	C(128,10,4,2,2)-GRU(76)-GRU(76)-FC(164)	199.8KB	7.6M	98.7%	93.2%	94.4%
CRNN	20	C(100,10,4,2,1)-GRU(136)-GRU(136)-FC(188)	499.5KB	19.3M	99.1%	94.4%	95.0%
DS-CNN	20	C(64,10,4,2,2)-DSC(64,3,1)-DSC(64,3,1)-DSC(64,3,1)-DSC(64,3,1)-AvgPool	38.6KB	5.4M	98.2%	93.6%	94.4%
DS-CNN	20	C(172,10,4,2,1)-DSC(172,3,2)-DSC(172,3,1)-DSC(172,3,1)-DSC(172,3,1)-AvgPool	189.2KB	19.8M	99.3%	94.2%	94.9%
DS-CNN	20	C(276,10,4,2,1)-DSC(276,3,2)-DSC(276,3,1)-DSC(276,3,1)-DSC(276,3,1)-DSC(276,3,1)-AvgPool	497.6KB	56.9M	99.3%	94.3%	95.4%

Table 7: Summary of hyperparameters of the best models described in Table 5.

Figures 9(a), 9(b), 9(c), 9(d) show the hyperparameter search of DNN, basic LSTM, LSTM and CRNN architectures depicting the model accuracy vs. number of operations. The model size is depicted by the size of the circle.

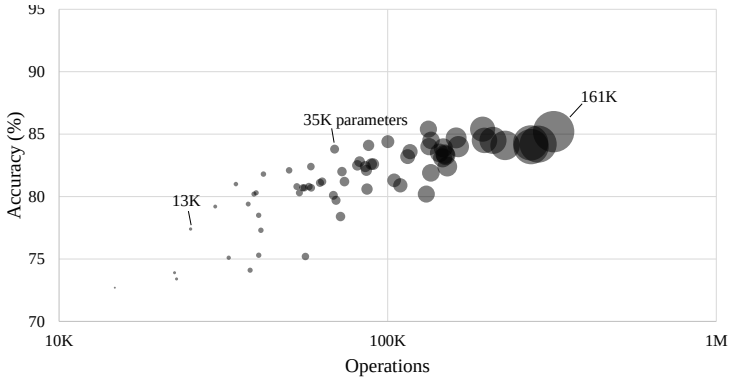

(a) DNN

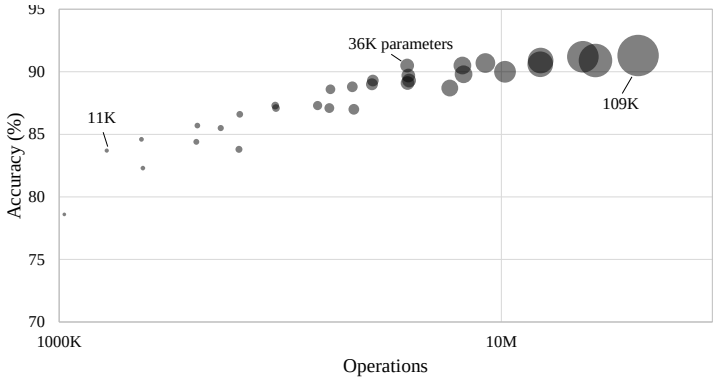

(b) Basic LSTM

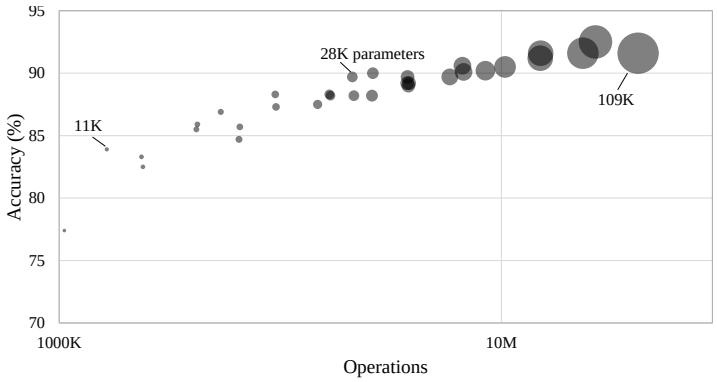

(c) LSTM

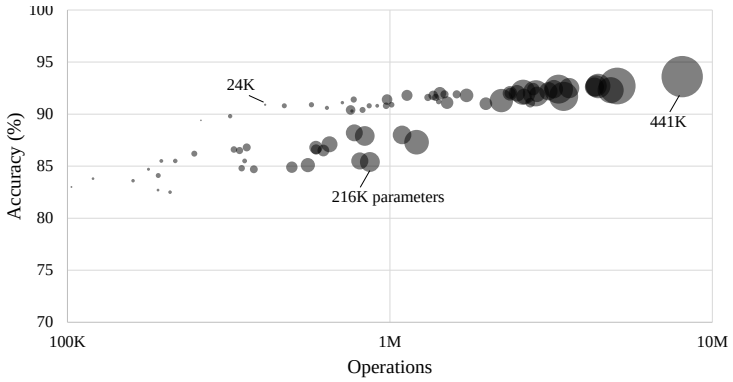

(d) CRNN

Figure 9: Hyperparameter search for (a) DNN, (b) basic LSTM, (c) LSTM and (d) CRNN showing the model accuracy vs. operations, with the number of parameters depicted by the size of the circle.